Chemistry & Biology
Brief Communication

Chemical Proteomics Identifies Nampt as the Target of CB30865, An Orphan Cytotoxic Compound

Tracey C. Fleischer,[1] Brett R. Murphy,[2] Jeffrey S. Flick,[1] Ryan T. Terry-Lorenzo,[1] Zhong-Hua Gao,[3] Thaylon Davis,[1] Rena McKinnon,[1] Kirill Ostanin,[1] J. Adam Willardsen,[2] and J. Jay Boniface[1,*]
[1]Department of Discovery Biology
[2]Department of Medicinal Chemistry
[3]Department of Research Services
Myriad Pharmaceuticals, 305 Chipeta Way, Salt Lake City, UT 84108, USA
*Correspondence: jay.boniface@myriadpharma.com
DOI 10.1016/j.chembiol.2010.05.008

SUMMARY

Drug discovery based on cellular phenotypes is impeded by the challenge of identifying the molecular target. To alleviate this problem, we developed a chemical proteomic process to identify cellular proteins that bind to small molecules. CB30865 is a potent (subnanomolar) and selective cytotoxic compound of previously unknown mechanism of action. By combining chemical proteomics with biochemical and cellular pharmacology we have determined that CB30865 cytotoxicity is due to subnanomolar inhibition of nicotinamide phosphoribosyltransferase (Nampt), an enzyme present in the NAD biosynthetic pathway. Cancer cells develop dependence on Nampt due to increased energy requirements and the elevated activity of NAD consuming enzymes such as sirtuins and mono and poly(ADP-ribose) polymerases (PARPs). These findings suggest new chemical starting points for Nampt inhibitors and further implicate this enzyme as a target in cancer.

INTRODUCTION

CB30865 (Figure 1A) is a subnanomolar cytotoxic compound discovered during the development of thymidylate synthase (TS) inhibitors as anticancer agents (Skelton et al., 1998, 1999). Using a quinazoline-based structural core, a series of pyridine containing compounds were synthesized (Skelton et al., 1998, 1999). Interestingly, although 2- and 4-pyridyl compounds exhibited cytotoxic potency consistent with their in vitro TS inhibitory activity, a 3-pyridyl analog, CB30865, was 100-fold more cytotoxic than would be anticipated by its in vitro potency (Skelton et al., 1998, 1999). A number of controls including the lack of rescue of cytotoxicity by addition of exogenous deoxythymidine indicated that CB30865 (Skelton et al., 1998, 1999) and its later analogs (Bavetsias et al., 2002) were acting on an additional target. In further protection studies CB30865 was not sensitive to the addition of a panel of metabolites (e.g., hypoxanthine, leucovorin, S-adenosine methionine, adenosine, guanosine, inosine, deoxycoformycin, methionine, and glycine) (Skelton et al., 1999). A COMPARE analysis of the cancer cell line cytotoxicity profile of CB30865 did not identify similarity to known antitumor agents, suggesting a novel mechanism of action (Skelton et al., 1999). Comparative genomic hybridization (Skelton et al., 1999) and comparative expressed sequence hybridization (Lu et al., 2001) identified an amplification on 7q22 in a CB30865-resistant cell line (W1L2:R8650). Microarray analysis implicated several candidate cDNAs in the region, but target identification was not reported (Lu et al., 2001). Testing a large panel of known chemotherapeutic agents for cross-resistance on the W1L2:R8650 versus the parental line was not insightful (Skelton et al., 1999). Thus, despite these efforts, the target of CB30865 has gone undetermined since its original description in 1998. In this work, we apply a chemical proteomics approach to identify the target of CB30865 and confirm its activity in both in vitro and mechanism-based cellular assays.

RESULTS

Chemical Compounds and Confirmation of Cytotoxicity

We synthesized a methylpiperazinyl derivative of CB30865, MPI-0479626 (Figure 1A), reported to have better solubility than the parent compound and to lack residual TS inhibition due to methylation of the 3-position of the quinazolinone ring (Bavetsias et al., 2002; Jones et al., 1985). Comparable to reported results, we found that MPI-0479626 was a potent cytotoxic compound, with an average TC_{50} of 0.7 nM in HCT116 cells (Figure 1B and Table 1). To serve as a negative control in subsequent experiments, we synthesized the corresponding 2-pyridyl analog, MPI-0482593 (Figure 1A). This compound was over 400-fold less potent in HCT116 cells than its 3-pyridyl isomer (Figure 1B and Table 1).

We next added a linker to enable affinity purification. Reported SAR (Bavetsias et al., 2002) indicated that the 2-position of the quinazolinone ring may be permissive to linker attachment. Therefore, an alkylamine linker was added to the methylpiperazine moiety of 3- and 2-pyridyl compounds, to yield MPI-0479883 and MPI-0482594, respectively (Figure 1A). MPI-0479883 had nanomolar cytotoxicity, suggesting that the linker did not severely compromise function (Table 1). Importantly,

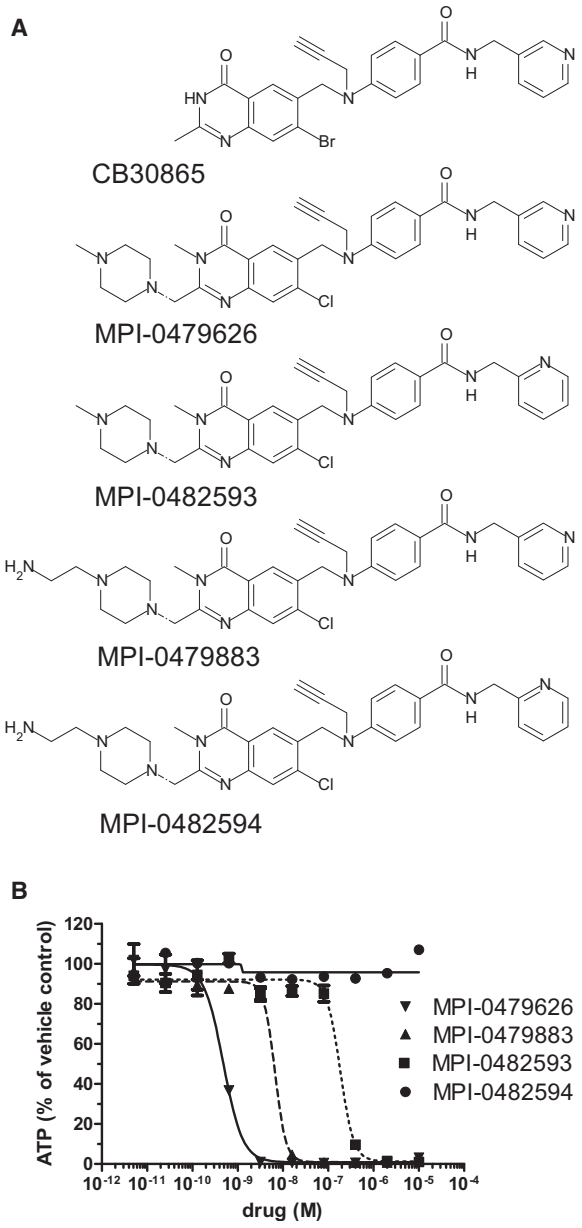

Figure 1. CB30865 Analogs Interact with Nampt

(A) Quinazolinone structures.

(B) Viability assay. Mean ATP levels of two replicates normalized to a vehicle control are plotted with the standard deviation.

the relative cellular potencies between the 2- and 3-pyridyl compounds were maintained on linker addition (Figure 1B and Table 1).

Small Molecule Affinity Purification

To identify candidate targets of CB30865, MPI-0479883 was immobilized on beads and incubated with a cell extract in the presence or absence of excess free compound as a competitor. As seen in the SDS-PAGE gel, a single prominent protein of ~55 kD was evident in the pull-down, but not with ethanolamine (EA) conjugated control beads or in the presence of competitor (Figure 2A).

We next analyzed the pull-downs by reversed-phase HPLC-tandem mass spectrometry (LC-MS/MS). The most abundant protein in the MPI-0479883 purification was Nampt (EC2.4.2.12), a 55 kD protein, which was not identified in either of the two negative controls (Figure 2B). Other associated proteins were substantially less abundant than Nampt and, with a few exceptions, were also present in the negative controls. Together, these data suggested that MPI-0479883 specifically interacted with Nampt.

Confirmation of the LC-MS/MS identification of Nampt as the 55 kD protein in MPI-0479883 pull-downs was done by immunoblotting for Nampt in aliquots of the same samples shown in Figure 2A. A single band was present in the Nampt immunoblot that migrated at ~55 kD (Figure 2C). Consistent with the MS and SDS-PAGE results, this band was absent in the EA control and competitor blocked pull-downs (Figure 2A).

To further address specificity, we compared the abundance of Nampt in MPI-0479883 pull-downs in the presence or absence of excess free 3- or 2-pyridyl competitors, (Figure 2D). The SDS-PAGE gel showed that MPI-0479883, but not MPI-0482594, effectively competed with immobilized MPI-0479883 for Nampt binding (Figure 2D). Consistent with the above, LC-MS/MS analyses on these samples indicated that spectral counts assigned to Nampt decreased by 86% with the 3-pyridyl competitor but only by 17% with the 2-pyridyl competitor (data not shown). Next, we compared the abundance of Nampt in purifications carried out with the 3- and 2-pyridyl compounds, MPI-0479883 and MPI-0482594, respectively. In these experiments, compounds were coupled to beads at different concentrations. By both SDS-PAGE and immunoblotting, MPI-0479883 specifically associated with Nampt, even when coupled at low densities (Figure 2E). In contrast, in MPI-0482594 pull-downs very little Nampt was detected even at the highest coupling density (Figure 2E). Together, these results are consistent with the 2-pyridyl compound having a lower affinity for Nampt and with the relative cellular potencies of CB30865 analogs.

Inhibition of Nampt In Vitro

In the first step of converting nicotinamide (NAM) to NAD, Nampt transfers a phosphoribosyl group from 5-phosphoribosyl-1-pyrophosphate (PRPP) to NAM, generating nicotinamide mononucleotide (NMN) (Rongvaux et al., 2002). To determine if CB30865 analogs are catalytic inhibitors of Nampt, we developed an in vitro assay for Nampt activity (Figure 3A). We observed dose-dependent inhibition with MPI-0479883 in this in vitro reaction (Figure 3B). A counter assay that bypassed Nampt and included NMN (shaded reactions, Figure 3A) confirmed that MPI-0479883 was exclusively inhibiting Nampt in the in vitro assay (Figure 3B). The average IC_{50} values from two experiments for MPI-0479626 and MPI-0479883 were 0.23 nM and 0.17 nM, respectively (Table 1). The 2-pyridyl compounds were significantly less potent Nampt inhibitors (Table 1), consistent with their diminished cytotoxicity. Two Nampt inhibitors, APO866 and GMX1778, have been or are currently in clinical trials for cancer (Holen et al., 2008; Hovstadius et al., 2002; Ravaud et al., 2005; von Heideman et al., 2009). As controls,

Table 1. Comparison of Nampt Inhibitor Potencies

Compound	Nampt Inhibition (IC_{50}, nM)	HCT116 Cytotoxicity (TC_{50}, nM)	NAD Depletion (IC_{50}, nM)	PAR Inhibition (IC_{50}, nM)
MPI-0479626	0.23 ± 0.12	0.68 ± 0.5	0.38 ± 0.08	0.08 ± 0.02
MPI-0479883	0.17 ± 0.03	19 ± 11	4.8 ± 3.4	1.8 ± 1.6
MPI-0482593	74 ± 2.1	280 ± 110	290 ± 68	47.0 ± 0.4
MPI-0482594	29 ± 2.8	>10,000	6200 ± 2000	3300 ± 1400
APO866	0.14 ± 0.04	1.4 ± 0.7	0.41 ± 0.30	0.38 ± 0.37
GMX1778	0.07 ± 0.03	2.3 ± 2.0	4.7 ± 3.4	0.77 ± 0.47

Shown are averages with the standard deviation from multiple independent experiments.

APO866 and GMX1778 were tested in the in vitro assay and both potently inhibited Nampt activity (Table 1).

Cellular Assays of Nampt Inhibition

We next tested the CB30865 derivatives and the established Nampt inhibitors in two cellular assays for Nampt activity. In both assays, we tested for the ability of the observed cellular effects to be prevented by exogenous nicotinic acid (NA), which cells convert into NAD via Nampt-independent pathways. First, we determined the levels of NAD-dependent PARP catalyzed nuclear poly(ADP) ribose (PAR) deposition. In the absence of a Nampt inhibitor, PAR was visible in the nucleus after exposure to the PARP activator H_2O_2 (Figure 3C). Addition of MPI-0479883 prevented the accumulation of nuclear PAR in the presence of H_2O_2 (Figure 3C). Quantification of the PAR signals from cells treated with different concentrations of MPI-0479883 revealed a dose-dependent decrease in nuclear PAR in response to MPI-0479883 that was prevented by addition of NA (Figure 3D).

As a second measure of Nampt cellular activity, we measured cellular NAD levels after a 24 hr incubation with Nampt inhibitors. MPI-0479883 gave a dose-proportional decrease in cellular NAD levels, whereas no decrease in NAD was seen in the presence of NA (Figure 3E). Under these conditions, there was no appearance of toxicity and no decrease in cellular ATP levels (data not shown).

Last, to confirm the on-target cytotoxicity of MPI-0479883 suggested by the mechanism based cellular assays, we tested if addition of NA was sufficient to prevent cytotoxicity associated

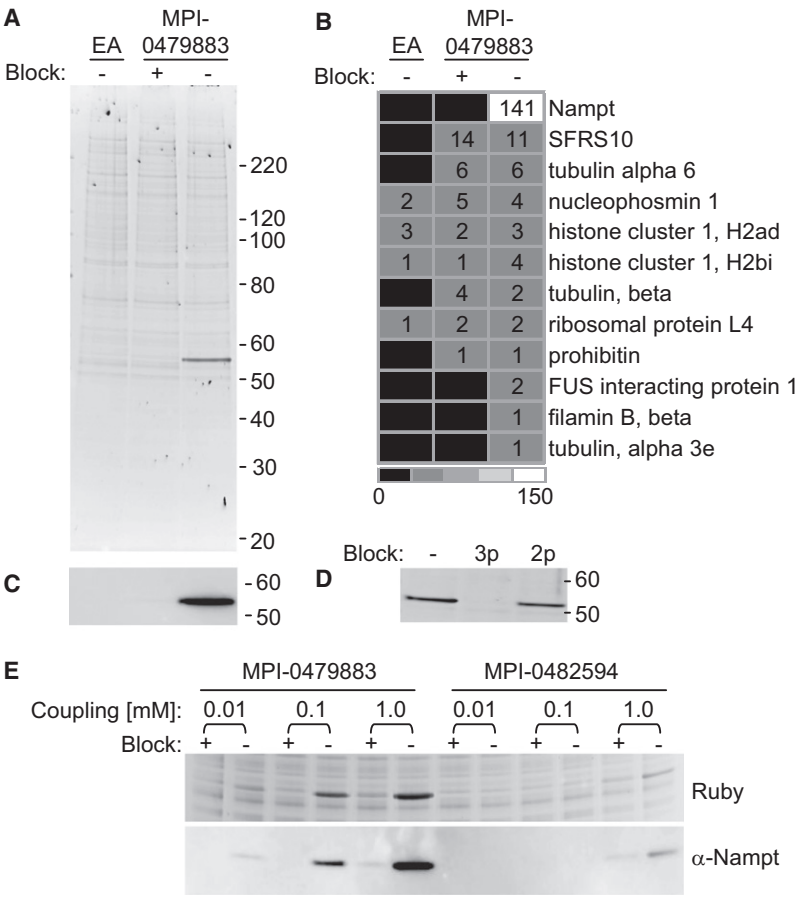

Figure 2. MPI-0479883 Interacts with Nampt

(A) MPI-0479883 affinity purification. SDS-PAGE gel showing pull-downs with EA- or MPI-0479883-beads in the presence (+) or absence (–) of 10 μM uncoupled MPI-0479883 (Block).

(B) LC-MS/MS analysis of pull-downs. The heat map indicates the total number of spectra corresponding to the listed proteins.

(C) α-Nampt immunoblot of pull-downs. Lanes are the same as in (A).

(D) Ruby-stained gel showing MPI-0479883 pull-downs blocked with vehicle (–), free MPI-0479883 (3p), or MPI-0482594 (2p).

(E) Ruby-stained gel and α-Nampt immunoblot of pull-downs done with MPI-0479883 or MPI-0482594 in the presence (+) or absence (–) of 10 μM of their respective free compound (Block). Density of compound was varied by coupling at the concentrations indicated.

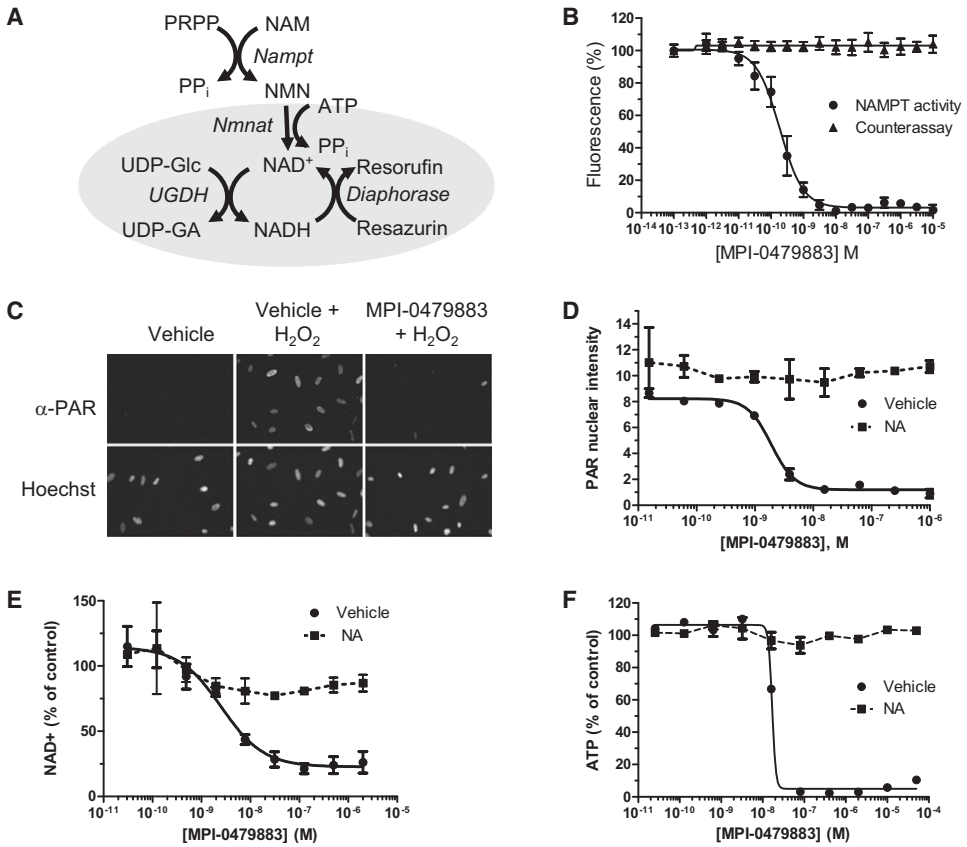

Figure 3. MPI-0479883 Inhibits Nampt Activity In Vitro and In Vivo

(A) Schematic of the in vitro Nampt assay.

(B) Dose response of MPI-0479883 in the Nampt assay. Graphs indicate average Nampt activity (resorufin fluorescence) normalized to a vehicle control. The standard deviation between duplicate samples is shown.

(C) PAR immunofluorescence assay. Cells treated with vehicle or MPI-0479883 and H_2O_2 where indicated were stained with α-PAR antibody and Hoechst to mark nuclei.

(D) The PAR intensity for cells treated with MPI-0479883 in the presence or absence of NA was quantified and the mean from duplicate experiments plotted with the standard deviation.

(E) NAD levels in cells treated with indicated amounts of MPI-0479883 in the presence (NA) or absence (vehicle) of 10 μM nicotinic acid. The mean and the standard error are shown.

(F) Cytotoxicity of MPI-0479883 in the absence (vehicle) or presence (NA) of 10 μM nicotinic acid. Mean ATP levels of two replicates normalized to a vehicle control are plotted with the standard deviation.

with Nampt inhibition. Indeed, cells given 10 μM NA retained viability in the presence of MPI-0479883, whereas in the absence of NA there was a dose-dependent loss of HCT116 cell viability (Figure 3F). It should be noted that in control experiments using a panel of cytotoxic agents, NA did not generally prevent cytotoxicity (data not shown). Together these results suggest that cytotoxicity of CB30865 is due to reduction in NAD through Nampt inhibition.

DISCUSSION

We describe the identification of the cellular target of CB30865, a highly potent cytotoxic orphan compound. Using small molecule affinity purification, only one protein, of approximately 55 kD, strongly and specifically interacted with MPI-0479883, a CB30865 analog. The LC-MS/MS analysis of the pull-down suggested the 55 kD protein was Nampt. The proteomic identification and specificity were further confirmed by immunoblotting pulldowns from 2- and 3-pyridyl isomers with a Nampt specific antibody.

After confirming the Nampt interaction, CB30865 analogs were shown to be potent inhibitors of Nampt activity in vitro and in mechanism-based cellular assays. TC_{50} values for cytotoxicity, the two cellular assays and in vitro potency can be compared in Table 1. Without exception, cytotoxicity and in vivo Nampt inhibition were completely blocked by NA (Figure 3 and data not shown). MPI-0479626 seems to be the most potent inhibitor of Nampt in cells, with subnanomolar cellular TC_{50} values. The addition of an ionizable amine linker to both 2- and 3-pyridyl compounds had little effect on in vitro potency, but diminished cellular potency, presumably due to effects on permeability. The published SAR (Skelton et al., 1998, 1999) for 3-pyridyl versus 2-pyridyl CB30865 analogs was in agreement with the relative potencies in all assays.

These consistencies in SAR and the complete prevention of cellular effects with NA strongly support Nampt inhibition as the molecular mechanism of cell killing for CB30865 and its analogs. It should be noted that the *nampt* gene is located in 7q22, the region amplified in the CB30865-resistant cell line, and evidence exists that increased levels of Nampt can render cells less sensitive to Nampt inhibition (Watson et al., 2009).

A common structural feature of Nampt inhibitors is the presence of a pyridine ring. In a Nampt cocrystal structure, the pyridyl moiety in APO866 has been shown to stack between the aromatic rings of Phe193 and Tyr18, functionally substituting for the pyridine ring present in the substrate, NAM, and product, NMN, of the enzymatic reaction (Khan et al., 2006; Kang et al., 2009). Molecular modeling based on the APO866-Nampt structure suggests that the pyridine in CB30865 can similarly stack (unpublished data), thus allowing the CB30865 derivatives to inhibit Nampt.

SIGNIFICANCE

We combined chemical proteomics with biochemical and cellular pharmacological approaches to unambiguously identify the target of an orphan molecule. The success of this approach suggests it will be applicable for target identification of other molecules with unknown mechanism of action. An activity responsible for conversion of NAM to NAD was described decades ago (Preiss and Handler, 1957), but it was not until 1994 that human *nampt* was cloned as a presumed cytokine called PBEF (Samal et al., 1994). That PBEF was Nampt became apparent with the cloning of a homologous gene in *Haemophilus ducreyi* that conferred NAD independence (Martin et al., 2001). Nampt activity was then confirmed for PBEF (Rongvaux et al., 2002). Consequently, only recently have the diverse biological functions of Nampt started to unfold (Gallí et al., 2010) and CB30865 analogs should become valuable tools in this regard. Concerning the clinical significance of these findings, there are currently two Nampt inhibitors in clinical trials in cancer (Holen et al., 2008; Hovstadius et al., 2002; Ravaud et al., 2005; von Heideman et al., 2009) and Nampt has been implicated in therapeutic areas outside of cancer as well (recently reviewed in Gallí et al., 2010; Borradaile and Pickering, 2009; Imai, 2009). The quinazolinone core of CB30865-like molecules, which is unique among Nampt inhibitors, may suggest new chemical starting points for future Nampt drug discovery efforts.

EXPERIMENTAL PROCEDURES

Chemical Syntheses

All compounds were synthesized with commercially available starting materials. See Supplemental Experimental Procedures (available online) for details.

Cytotoxicity Assay

HCT116 cells (ATCC) were seeded at 5000 cells per well in 96-well plates. Indicated amounts of compound and 10 μM NA, where applicable, were added to cells for 72 hr. Viability was measured with the CellTiter-Glo Luminescent Cell Viability Assay (Promega) according to manufacturer's instructions. Luminescence was measured using a TopCount NXT plate reader (Perkin-Elmer).

Small Molecule Affinity Purification

Compounds containing an ethylamine linker were immobilized on beads and incubated with cell lysates (see Supplemental Experimental Procedures). Where indicated, excess free compound was added to the lysates before adding the immobilized compound. Interacting proteins were pulled down and analyzed by SDS-PAGE and LC-MS/MS.

Liquid Chromatography–Mass Spectrometry

Proteins were reduced, alkylated, and digested with trypsin directly on the beads. Tryptic peptides were separated by nano-flow microcapillary reversed-phased HPLC and eluted directly into an LTQ-Orbitrap (Thermo Fisher). For each full scan the top five most abundant ions were fragmented. Peptides and proteins were identified with Sequest (Eng et al., 1994) and hierarchical clustering was done using BIGCAT (McAfee et al., 2006). See Supplemental Experimental Procedures for details.

Nampt Assay

PRPP, ATP, NAM, NMN, Triton X-100, UDP-glucose, and diaphorase were purchased from Sigma. Human *nampt*, NMN adenylyltransferase (*nmnat1*), and UDP-glucose dehydrogenase (*ugdh*) genes were inserted into a house-modified *Escherichia coli* expression vector with an N-terminal 6xHis tag. Protein expression in BL21-AI *E. coli* (Invitrogen) was induced by 0.2% L-arabinose and 0.5 mM IPTG at 30°C. Proteins were purified on Ni-NTA resin (QIAGEN), according to manufacturer's instructions.

The Nampt assay was run in real-time mode in 96-well plates using 50 mM Tris-HCl, pH 7.5, 1% DMSO (v/v), 0.01% Triton X-100 (v/v), 10 mM $MgCl_2$, 2 mM ATP, 3 μM NAM, 8 μM PRPP, 50 pM Nampt, 5 nM Nmnat, 200 nM Ugdh, 200 μM UDP-glucose, 0.02 U/ml diaphorase, and 0.25 μM resazurin. Reactions were incubated at room temperature for up to 3 hr and then fluorescence at excitation and emission wavelengths of 510 nm and 590 nm, respectively, was measured using a Gemini XS plate reader (Molecular Devices). The counter assay was run as above, but with 1 μM NMN substituting for Nampt.

PAR Assay

MCF-10A cells (ATCC) stably transduced with the oncogene encoding PIK3-CA(H1047R) were seeded at 6000 cells/well in 96-well plates. Compound was added for 20–24 hr. Hydrogen peroxide (500 μM) was added for 8 min and cells were fixed in 100% −20°C methanol. After washing with PBS, cells were incubated in blocking buffer (HBSS, 1% BSA, 0.1% Tween20) then stained with an α-PAR mouse monoclonal antibody (Trevigen, 1:2000). For detection, 1:1000 of α-mouse-Alexa488 and 5 μg/mL Hoechst 33342 were used (Invitrogen). Images were acquired on a Pathway 855 (BD Biosciences) using a 10× objective. Using Attovision software (BD Biosciences), the Hoechst signal was used to segment nuclei and the PAR signal for each nucleus in a well was subsequently averaged to generate a single value.

Assay to Measure NAD in Cellular Lysates

MCF-10A cells stably transduced with the oncogene encoding PIK3-CA(H1047R) were treated with compound for 20–24 hr. Cells were washed in PBS, lysed in 25 μl 0.5 M perchloric acid, and neutralized with 8 μl of 2 M KOH/0.2 M K_2HPO_4. After clearing the precipitate by centrifugation, 10 μl lysate was added to 90 μl of reaction (final concentration of 120 μM Tris-HCl, pH 7.5, 0.01% Triton X-100, 35 μM UDP-Glucose, 50 nM Ugdh, 0.5 μM resazurin, and 0.1 unit/mL diaphorase) for 1 hr at room temperature. Fluorescence was read as for Nampt inhibition.

SUPPLEMENTAL INFORMATION

Supplemental information includes Supplemental Experimental Procedures and can be found with this article online at doi:10.1016/j.chembiol.2010.05.008.

ACKNOWLEDGMENTS

We gratefully acknowledge D. Wettstein for discussions related to deorphaning compounds using chemical proteomics, M. Shenderovich for molecular modeling, S. Ghaffari for technical assistance, A. Gassman for critical

comments on the manuscript, and R. Carlson for support. All authors are or were employees of Myriad Pharmaceuticals, Inc.

Received: March 23, 2010
Revised: May 5, 2010
Accepted: May 7, 2010
Published: June 24, 2010

REFERENCES

Bavetsias, V., Skelton, L.A., Yafai, F., Mitchell, F., Wilson, S.C., Allan, B., and Jackman, A.L. (2002). The design and synthesis of water-soluble analogues of CB30865, a quinazolin-4-one-based antitumor agent. J. Med. Chem. *45*, 3692–3702.

Borradaile, N.M., and Pickering, J.G. (2009). NAD(+), sirtuins, and cardiovascular disease. Curr. Pharm. Des. *15*, 110–117.

Eng, J., McCormack, A., and Yates, J.R. (1994). An approach to correlate tandem mass spectral data of peptides with amino acid sequences in a protein database. J. Am. Soc. Mass Spectrom. *5*, 976–989.

Gallí, M., Van Gool, F., Rongvaux, A., Andris, F., and Leo, O. (2010). The nicotinamide phosphoribosyltransferase: a molecular link between metabolism, inflammation, and cancer. Cancer Res. *70*, 8–11.

Holen, K., Saltz, L.B., Hollywood, E., Burk, K., and Hanauske, A.R. (2008). The pharmacokinetics, toxicities, and biologic effects of FK866, a nicotinamide adenine dinucleotide biosynthesis inhibitor. Invest. New Drugs *26*, 45–51.

Hovstadius, P., Larsson, R., Jonsson, E., Skov, T., Kissmeyer, A.M., Krasilnikoff, K., Bergh, J., Karlsson, M.O., Lönnebo, A., and Ahlgren, J. (2002). A Phase I study of CHS 828 in patients with solid tumor malignancy. Clin. Cancer Res. *8*, 2843–2850.

Imai, S. (2009). Nicotinamide phosphoribosyltransferase (Nampt): a link between NAD biology, metabolism, and diseases. Curr. Pharm. Des. *15*, 20–28.

Jones, T.R., Calvert, A.H., Jackman, A.L., Eakin, M.A., Smithers, M.J., Betteridge, R.F., Newell, D.R., Hayter, A.J., Stocker, A., Harland, S.J., et al. (1985). Quinazoline antifolates inhibiting thymidylate synthase: variation of the N10 substituent. J. Med. Chem. *28*, 1468–1476.

Kang, G.B., Bae, M.H., Kim, M.K., Im, I., Kim, Y.C., and Eom, S.H. (2009). Crystal structure of *Rattus norvegicus* Visfatin/PBEF/Nampt in complex with an FK866-based inhibitor. Mol. Cells *27*, 667–671.

Khan, J.A., Tao, X., and Tong, L. (2006). Molecular basis for the inhibition of human NMPRTase, a novel target for anticancer agents. Nat. Struct. Mol. Biol. *13*, 582–588.

Lu, Y.J., Williamson, D., Clark, J., Wang, R., Tiffin, N., Skelton, L., Gordon, T., Williams, R., Allan, B., Jackman, A., et al. (2001). Comparative expressed sequence hybridization to chromosomes for tumor classification and identification of genomic regions of differential gene expression. Proc. Natl. Acad. Sci. USA *98*, 9197–9202.

Martin, P.R., Shea, R.J., and Mulks, M.H. (2001). Identification of a plasmid-encoded gene from *Haemophilus ducreyi* which confers NAD independence. J. Bacteriol. *183*, 1168–1174.

McAfee, K.J., Duncan, D.T., Assink, M., and Link, A.J. (2006). Analyzing proteomes and protein function using graphical comparative analysis of tandem mass spectrometry results. Mol. Cell. Proteomics *5*, 1497–1513.

Preiss, J., and Handler, P. (1957). Enzymatic synthesis of nicotinamide mononucleotide. J. Biol. Chem. *225*, 759–770.

Rongvaux, A., Shea, R.J., Mulks, M.H., Gigot, D., Urbain, J., Leo, O., and Andris, F. (2002). Pre-B-cell colony-enhancing factor, whose expression is up-regulated in activated lymphocytes, is a nicotinamide phosphoribosyltransferase, a cytosolic enzyme involved in NAD biosynthesis. Eur. J. Immunol. *32*, 3225–3234.

Ravaud, A., Cerny, T., Terret, C., Wanders, J., Bui, B.N., Hess, D., Droz, J.P., Fumoleau, P., and Twelves, C. (2005). Phase I study and pharmacokinetic of CHS-828, a guanidino-containing compound, administered orally as a single dose every 3 weeks in solid tumors: an ECSG/EORTC study. Eur. J. Cancer *41*, 702–707.

Samal, B., Sun, Y., Stearns, G., Xie, C., Suggs, S., and McNiece, I. (1994). Cloning and characterization of the cDNA encoding a novel human pre-B-cell colony-enhancing factor. Mol. Cell. Biol. *14*, 1431–1437.

Skelton, L.A., Ormerod, M.G., Titley, J.C., and Jackman, A.L. (1998). Cell cycle effects of CB30865, a lipophilic quinazoline-based analogue of the antifolate thymidylate synthase inhibitor ICI 198583 with an undefined mechanism of action. Cytometry *33*, 56–66.

Skelton, L.A., Ormerod, M.G., Titley, J., Kimbell, R., Brunton, L.A., and Jackman, A.L. (1999). A novel class of lipophilic quinazoline-based folic acid analogues: cytotoxic agents with a folate-independent locus. Br. J. Cancer *79*, 1692–1701.

von Heideman, A., Berglund, A., Larsson, R., and Nygren, P. (2009). Safety and efficacy of NAD depleting cancer drugs: results of a phase I clinical trial of CHS 828 and overview of published data. Cancer Chemother. Pharmacol. *65*, 1165–1172.

Watson, M., Roulston, A., Bélec, L., Billot, X., Marcellus, R., Bédard, D., Bernier, C., Branchaud, S., Chan, H., Dairi, K., et al. (2009). The small molecule GMX1778 is a potent inhibitor of NAD^+ biosynthesis: strategy for enhanced therapy in nicotinic acid phosphoribosyltransferase 1-deficient tumors. Mol. Cell. Biol. *29*, 5872–5888.

